BIBECHANA
Vol. 20, No. 3, December 2023, 328–335

ISSN 2091-0762 (Print), 2382-5340 (Online)
Journal homepage: http://nepjol.info/index.php/BIBECHANA
Publisher:Dept. of Phys., Mahendra Morang A. M. Campus (Tribhuvan University)Biratnagar

Thermodynamic, structural and surface properties of Cu–Zr liquid alloy at different temperatures: A theoretical approach

Shashit Kumar Yadav*, Dipak Rohita Yadav, Ramesh Kumar Gohivar, Upendra Mehta

Department of Physics, Mahendra Morang Adarsh Multiple Campus, Tribhuvan University
Biratnagar, Nepal.

*Corresponding author. Email: yadavshashit@yahoo.com

Abstract

Quasi-lattice model has been employed to study the thermodynamic and microscopic structural properties of Cu–Zr liquid alloy in the temperature range 1400-1700 K. The model fit parameters required for the purpose have been optimised using the available literature data of thermodynamic properties at the melting temperature of the system, 1400 K. These model parameters have been then computed at different temperatures assuming them to be linear temperature-dependent. The surface properties of the system have been computed using Butler model at above mentioned temperatures.

Keywords
Quasi–lattice test, ordering nature, segregating nature, surface tension.

Article information
Manuscript received: August 10, 2023; Revised: September 27, 2024; Accepted: October 1, 2023
DOI https://doi.org/10.3126/bibechana.v21i3.70438

1 Introduction

Pure metals are inappropriate for the most of industrial uses as they are often soft and ductile. As a result, alloying is done to produce desirable composite material with low to high melting points, increased tensile strength, improved corrosion resistance and greater cost accessibility [1]. They are used in culinary utensils, automobile parts, aerospace parts, cellphone parts, medicines, military, nuclear reactors, etc. Therefore, alloying phenomenon is incredibly crucial in our daily lives [2]. Alloys of Cu–Zr have a relatively weak interaction [3] and tend to pass into the glassy state over a wide composition range. In this regard, they are used as the foundation for a wide range of bulk amorphous materials. The long-term operation of nuclear reprocessing plants is jeopardized by the management of zirconium base alloy wastes as cladding hulls [4]. Hence, the system has been studied by several researchers employing different experimental techniques and

theoretical approaches.

The Butler Model was used to study the surface characteristics of the system above its melting point [5]. In 2003, Zaitsev et al. produced a full experimental thermodynamic description of Cu-Zr intermetallic complexes [3]. The knowledge of phase diagram and thermodynamic parameters including enthalpy of mixing, enthalpy of formation and heat contents are required for the purpose. The information for glass forming propensity requires knowledge of the thermodynamic and kinetic parameters of Cu–Zr alloys [4]. In 2008, Yamaguchi et al. evaluated the standard enthalpy of formation of Cu_9Zr_2, $Cu_{51}Zr_{14}$, Cu_8Zr_3, $Cu_{10}Zr_7$, and $CuZr_2$ complexes at 298.15 K [2]. The present literature review shows that the complete assessment of mixing properties of the system in liquid state is not available to date.

Therefore, the thermodynamic and structural properties of the Cu–Zr liquid alloy at 1400 K have been studied in the work on the basis of quasi-lattice test [6–10]. The model parameters required for the process have been optimised taking the thermodynamic data of ref. [11] as reference. The calculated values of thermodynamic and structural properties have been then compared with the reference data to check the validity of best fit values of so obtained model parameters. The surface tension and surface concentrations of components in the alloy have been computed using Butler model [10, 12–14]. In order to analyse the mixing tendency of the system at higher temperatures, above mentioned properties have been calculated in the temperature range 1400-1700 K.

2 Formalism

2.1 Thermodynamics properties

The complex having the stiochiometric composition $A_\mu B, \mu = 2$, i.e., Zr_2Cu [11] has been assumed to be energetically stable in the alloy. According to the quasi-lattice model, the expression for excess free energy of mixing (ΔG_M^{xs}) for the preferred complex is given as [6–10]

$$\Delta G_M^{\text{xs}} = N\left[\Delta\omega\phi + \Delta\omega_{\text{AB}}\phi_{\text{AB}} + \Delta\omega_{\text{AA}}\phi_{\text{AA}}\right] \quad (1)$$

where

$$\phi = x_1 x_2 \quad (2a)$$

$$\phi_{\text{AB}} = \left(\frac{1}{6}x_1 + {x_1}^2 - \frac{5}{3}{x_1}^3 + \frac{1}{2}{x_1}^4\right) \quad (2b)$$

$$\phi_{\text{AA}} = \left(-\frac{1}{4}x_1 + \frac{1}{2}{x_1}^2 - \frac{1}{4}{x_1}^4\right) \quad (2c)$$

And the expression for free energy of mixing is given by

$$\Delta G_M = \Delta G_M^{\text{xs}} + RT\left[x_1 \ln x_1 + x_2 \ln x_2\right] \quad (3)$$

Herein, $\Delta\omega$ and $\Delta\omega_{ij}; i, j = A, B$ are the interaction energy parameters, termed as model parameters. R is the real gas constant and T is the absolute temperature. $x_i, i = A, B$ is the mole fraction of pure component i in the liquid alloy.

Let a_A and a_B denote the activities of the elements A (=Zr) and B(=Cu) in the alloy. a_A and a_B can be expressed as

$$\text{RT} \ln a_A = \Delta G_M + x_2 \left(\frac{\partial \Delta G_M}{\partial x_1}\right)_{T,P,N} \quad (4)$$

and

$$\text{RT} \ln a_B = \Delta G_M + x_1 \left(\frac{\partial \Delta G_M}{\partial x_2}\right)_{T,P,N} \quad (5)$$

The expression for the excess entropy of mixing (ΔS_M^{xs}) can be expressed in terms of ΔG_M^{xs} with the help of standard thermodynamic relation as

$$\Delta S_M^{\text{xs}} = -\left(\frac{\partial \Delta G_M^{\text{xs}}}{\partial T}\right)_P \quad (6)$$

Using Equation (2) in Equation (6), one can obtain

$$\Delta S_M^{\text{xs}} = -N\left[\frac{\partial \Delta\omega}{\partial T}\phi + \frac{\partial \Delta\omega_{AB}}{\partial T}\phi_{AB} + \frac{\partial \Delta\omega_{AA}}{\partial T}\phi_{AA}\right] \quad (7)$$

where $\frac{\partial \Delta\omega}{\partial T}$ and $\frac{\partial \Delta\omega_{ij}}{\partial T}$ are the temperature derivative terms of interaction energy parameters.

The enthalpy of mixing (ΔH_M), ΔS_M^{xs} and ΔG_M^{xs} can be related as

$$\Delta H_M = \Delta G_M^{\text{xs}} + T\Delta S_M^{\text{xs}} \quad (8)$$

2.2 Structural properties

The arrangement of atoms in the liquid alloys can be studied by calculating characteristics functions, such as concentration fluctuation in the long wave length limit ($S_{CC}(0)$), Warren-Cowley short range order parameter (α_1) and the ratio of mutual to intrinsic diffusion coefficients (D_M/D_{id}) [6, 7, 15, 16]. $S_{CC}(0)$ can be expressed in terms of ΔG_M as

$$S_{CC}(0) = \text{RT}\left[\frac{\partial^2 \Delta G_M}{\partial {x_i}^2}\right]^{-1}_{T,P,N} \quad (9)$$

With the aid Equations (2 and 3) in Equation (2.2), $S_{CC}(0)$ can be expressed as

$$S_{CC}(0) = x_1 x_2 * P^{-1}$$

with

$$P = 1+x_1x_2\mathrm{RT}\left(\Delta\omega\phi" + \Delta\omega_{AB}\phi"_{AB} + \Delta\omega_{AA}\phi"_{AA}\right) \quad (10)$$

Moreover, the expression for ideal value of concentration fluctuation in long wavelenth limit $S^{\mathrm{id}}_{cc}(0)$ as

$$S^{id}_{cc}(0) = x_1x_2 \quad (11)$$

As sated above, another structural function, α_1 can be expressed as [15, 17, 18]

$$\alpha_1 = \frac{S-1}{[S(Z-1)+1]} \quad (12)$$

Here, Z represents the coordination number and its value has been taken to be 10 for the work. The term S in above expression is defined as

$$S = \frac{S_{CC}(0)}{S^{\mathrm{id}}_{CC}(0)} \quad (13)$$

The ratio of mutual to intrinsic diffusion coefficients is expressed as [9, 19]

$$\frac{D_M}{D_{\mathrm{id}}} = \frac{S^{\mathrm{id}}_{CC}(0)}{S_{CC}(0)} \quad (14)$$

2.3 Surface properties

The knowledge of surface tension and surface segregation allows us to understand and explain the mechanical behavior, phase change, catalytic activity, and other physical behaviours of an alloy . The expression for the surface tension (σ) for binary liquid alloy is given as [12, 20–22]

$$\sigma = \sigma^0_1(T) + \frac{RT}{A_1}\ln\left(\frac{x^s_1}{x_1}\right) + \left(\frac{\Delta G^{\mathrm{xs},s}_1 - \Delta G^{\mathrm{xs},b}_1}{A_1}\right)$$

$$\sigma = \sigma^0_2(T) + \frac{RT}{A_2}\ln\left(\frac{x^s_2}{x_2}\right) + \left(\frac{\Delta G^{\mathrm{xs},s}_2 - \Delta G^{\mathrm{xs},b}_2}{A_2}\right) \quad (15)$$

where A_i = molar surface area of i^{th} component, x^s_i = surface mole fraction of the i^{th}component, x_i= bulk mole fraction of i^{th} component, $\Delta G^{\mathrm{xs},s}_i$ = partial excess free energy of the i^{th} component in the surface phase of liquid solution and $\Delta G^{\mathrm{xs},b}_i$ = partial excess free energy of the i^{th} component in the liquid solution. $\Delta G^{\mathrm{xs},s}_i$ and $\Delta G^{\mathrm{xs},b}_i$ is related by the expression

$$\Delta G^{\mathrm{xs},s}_i = \beta\Delta G^{\mathrm{xs},b}_i \quad (16)$$

The value of β depends on the ratio of coordination number of atoms in surface phase and bulk phase. The value of β is taken to be 0.8181 [10, 13, 20] in the work.

In Equation (12), $\sigma^0_i(T)$ is the temperature dependent surface tension of pure i^{th} component in the mixture that can be expressed as [14, 23]

$$\sigma^0_i(T) = \sigma^0_i + (T - T_0)\frac{d\sigma}{dT} \quad (17)$$

The terms σ^0_i is the surface tension of pure component at its melting temperature (T_0), $\sigma^0_i(T)$ is the surface tension at the required temperature T, and $\frac{d\sigma}{dT}$ is the temperature derivative term of surface tension. The expression of the molar surface area of the i^{th} component can be given by [10, 13]

$$A_i = f(V^0_i)^{2/3}(N_{AV})^{1/3} \quad (18)$$

The terms V_i and N_{AV} are the molar volume of i^{th} component at temperature T and Avogadro's number respectively. The term f is geometrical constant and its value is 1.000 that can be calculated using the relation [21, 24]

$$f = \left(\frac{3f_b}{4}\right)\frac{\pi^{1/3}}{f_s} \quad (19)$$

Herein,f_b and f_s are the volume and surface packing fractions. The ideal surface tension of the binary alloy is the weighted sum of surface tension of individual components present in the alloy. Mathematically,

$$\sigma^{\mathrm{id}} = \sigma^0_1(T)x_1 + \sigma^0_2(T)x_2 \quad (20)$$

where the terms carry their usual meanings as stated above.

3 Results and discussion

3.1 Thermodynamic properties

The model parameters required for the quasi-lattice test, have been obtained by considering the thermodynamic database of Cost 507 [11] as reference. The self-consistent parameters for ΔG^{xs}_M is expressed in terms of coefficients of Redlich-Kister polynomial [25] in the ref. [11], Table 1.

Table 1: Interaction energy parameters for ΔG^{xs}_M

Parameters [Jmol^{-1}]	Ref.
$L_0 = -61685.53 + 11.29235 * T$ $L_1 = 8830.66 + 5.045658 * T$	[11]
$\Delta\omega = -43271.6 + 15.680 * (T - 1400)$ $\Delta\omega_{AB} = 3776.065 + 1.200 * (T - 1400)$ $\Delta\omega_{AA} = 65496.02 + 0.010 * (T - 1400)$	This wok

ΔG^{xs}_M for the system in terms of coefficients of R-K polynomial can be expressed as [9, 10, 25]

$$\Delta G^{\mathrm{xs}}_M = x_1x_2\left(L_0 + L_1(x_1 - x_2)\right) \quad (21)$$

where L_i (in Jmol^{-1}is the coefficient of R-K polynomial depending on temperature but independent

of concentration. $L_i = a_i + b_i * T$, where a_i is the contribution of enthalpy of mixing ΔH_M and b_i is the contribution of entropy of mixing (ΔS_M^{xs}) on ΔG_M^{xs}. The expressions of ΔS_M^{xs} and ΔH_M then can be obtained using the Equations (6 and 8) as [9]

$$\Delta S_M^{xs} = x_1 x_2 \left[b_0 + b_1(x_1 - x_2)\right] \quad (22)$$

and

$$\Delta H_M = x_1 x_2 \left[a_0 + a_1(x_1 - x_2)\right] \quad (23)$$

The reference values of ΔG_M^{xs}, ΔH_M and ΔS_M^{xs} have been calculated using Equations (21-23) with the help of parameters in Table 1. The values of model parameters $\Delta\omega$, $\Delta\omega_{AB}$ and $\Delta\omega_{AA}$ and their temperature derivative terms ($\frac{\partial\Delta\omega}{\partial T}$, $\frac{\partial\Delta\omega_{AB}}{\partial T}$ and $\frac{\partial\Delta\omega_{AA}}{\partial T}$) at 1400 K have been then optimised by using Equations (1,2, 7 and 8) and calculated reference values of ΔG_M^{xs}, ΔH_M and ΔS_M^{xs}. The best best fit values of these model parameters are presented in Table 1. These model parameters are also assumed to depend only on temperature. The calculated values of these thermodynamic functions are plotted in Figure 1.

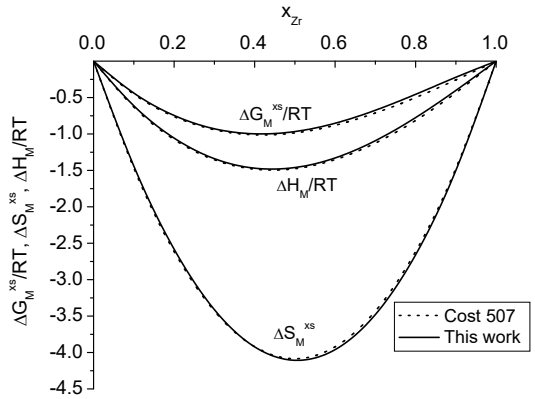

Figure 1: Plot of ΔG_M^{xs} versus x_{Zr} for Cu–Zr liquid alloy at 1400 K.

The values of ΔG_M^{xs}, ΔH_M and ΔS_M^{xs} calculated using the optimised parameters of the work and Cost 507 [11] are found to be consistent with each other at its melting temperature, 1400 K. The negative values of ordering energy parameter, $\Delta\omega$, signifies the compound forming behavior of the system at its melting temperature. The optimum value of $\Delta G_M^{xs} = -11612.8$ Jmol^{-1} and $\Delta H_M = -17104.0$ Jmol^{-1} at $x_{xs} = 0.4$, indicating the system to be asymmetric with respect to these functions, Figure 1. Moreover, the system is found to be weakly interacting in nature.

The values of ΔG_M^{xs} of the system have also been computed at higher temperatures, 1400 K, 1500 K, 1600 K and 1700 K following the similar procedure. The calculated optimum values of ΔG_M^{xs} at x_{Zr} are -11612.8 Jmol^{-1} at 1400 K, $- - 11220.6$ Jmol^{-1} at 1500 K, -10828.4 Jmol^{-1} at 1600 K and -10436.1 Jmol^{-1} at 1700 K. Thus, the negative values of ΔG_M^{xs} are found to gradually decrease with an increase in the temperature of the system, Figure 2. These results indicate that the compound forming tendency in the liquid alloy gradually decreases with an increase in its temperature.

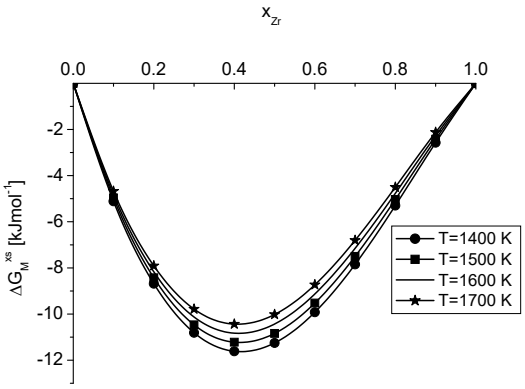

Figure 2: Calculated values of a_{Zr} and a_{Cu} versus x_{Zr} for Cu–Zr liquid alloy at 1400 K.

Activity is another important thermodynamic parameter which is greatly influenced by the values of model parameters and is reflection of ΔG_M^{xs}. The activities of components Zr (a_{Zr}) and Cu (a_{Cu}) of liquid alloy have been calculated using Equations (4, 5 and 21) with the aid of parameters in Table 1.

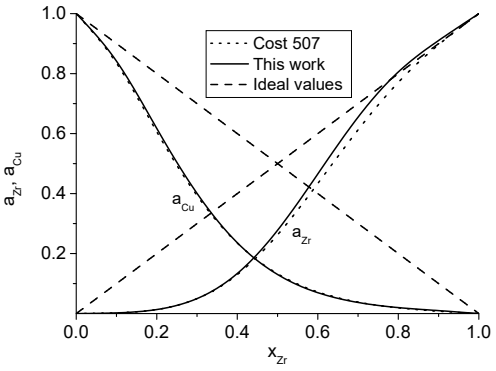

Figure 3: Calculated values of a_{Zr} and a_{Cu} versus x_{Zr} for Cu–Zr liquid alloy at 1400 K.

The perusal of Figure 3 conveys that the calculated values of a_{Zr} and a_{Cu} using the model parameters of the work are found to be consistent with those calculated using the data of Cost 507 [11]. The activities of these components show negative deviation from Raoult's law or their respective ideal values

at lower concentrations of Zr indicating the system to be ordering in nature. However, values of a_{Zr} approaches ideal values at higher concentration of Zr.

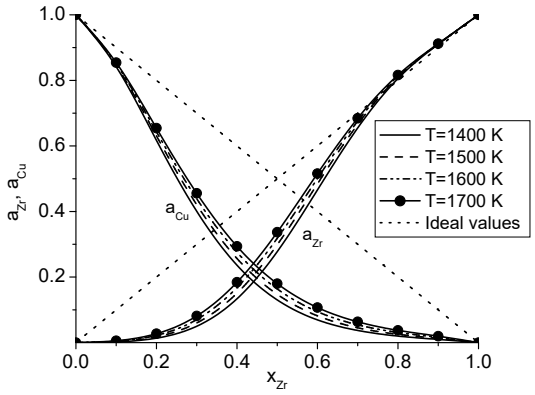

Figure 4: Calculated values of a_{Zr} and a_{Cu} as a function of concentration of Zr for Cu–Zr liquid alloy at different temperatures.

The activity of the system has also been computed at above mentioned different temperatures. The calculated values of a_{Zr} and a_{Cu} are found to gradually increase at higher temperatures, Figure 4. The deviation of calculated values from the ideal values gradually decreases. The activity of the component Zr shows positive deviation from its respective ideal value at 1500 K and above in the concentration range $x_{\mathrm{Zr}} > 0.8$. These results correspond the transformation from ordering to segregating nature of the system. Thus, the present investigations reveal that the compound forming tendency in the alloy decreases at elevated temperatures.

3.2 Structural properties

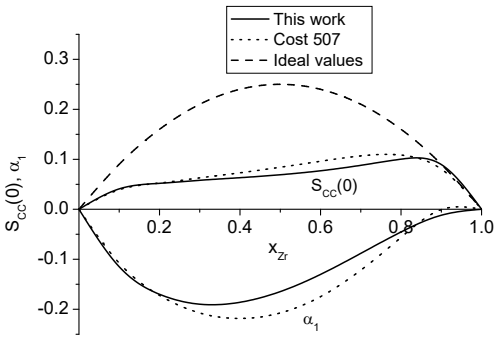

Figure 5: Calculated values of $S_{CC}(0)$ and α_1 versus x_{Zr} for Cu–Zr liquid alloy at 1400 K.

The ordering nature or hetero-atomic pairing and segregating nature or homo-atomic pairing tendencies in the liquid alloys can be better understood with the knowledge of microscopic structural functions. For the purpose, concentration fluctuation in long wavelength limit ($S_{CC}(0)$), Warren-Cowley short-range order parameter (α_1) and ratio of mutual to intrinsic diffusion coefficients (D_M/D_{id}) have been computed in the work using Equations (9-14) and parameters in Table 1.

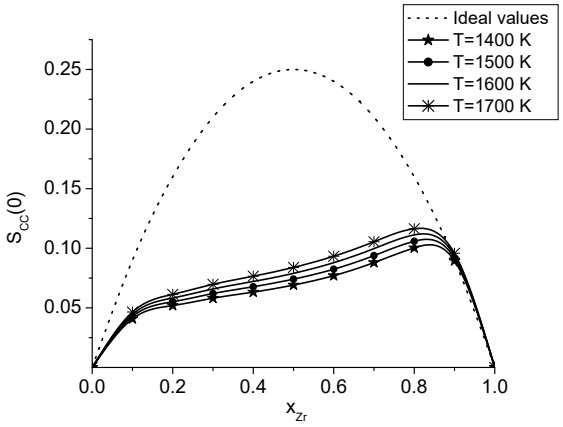

Figure 6: Calculated values of $S_{CC}(0)$ versus x_{Zr} for Cu–Zr liquid alloy at different temperatures.

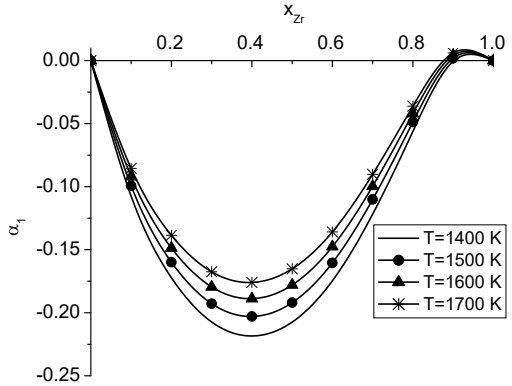

Figure 7: Calculated values of α_1 versus x_{Zr} for Cu–Zr liquid alloy at different temperatures.

At a given concentration and temperature, if $S_{CC}(0) > S^{\mathrm{id}}_{CC}$, then it indicates ordering tendency in the alloy for which $\alpha_1 > 1$ and $D_M/D_{\mathrm{id}} < 1$. Likewise, if $S_{CC}(0) < S^{\mathrm{id}}_{CC}$, then it indicates segregating tendency in the alloy for which $\alpha_1 < 1$ and $D_M/D_{\mathrm{id}} > 1$. If $\alpha_1 = 0$, then ideal mixing tendency in the liquid alloy is expected. The calculated values of $S_{CC}(0) < S^{\mathrm{id}}_{CC}$ and $\alpha_1 < 1$ in the entire concentration range indicating the ordering

nature of the system, Figure 5. Moreover, values of these functions computed using the optimised coefficients of the work are found to be in reasonable agreement with those obtained using the parameters of Cost 507 [11].

The values of $S_{CC}(0)$ are also calculated at higher temperatures following the similar procedure as mentioned above. $S_{CC}(0)$ gradually increases with an increase in temperature of the system and approaches ideal values, Figure 6. The calculated values of $S_{CC}(0)$ are found to be grater than ideal values in the concentration range $x_{\mathrm{Zr}} > 0.8$ at T>1400 K. Thus, it can be stated that the system changes from ordering to segregating nature at these conditions. Likewise, the calculated values of α_1 is found to be greater than 1 in the above mentioned conditions revealing the similar mixing tendency.

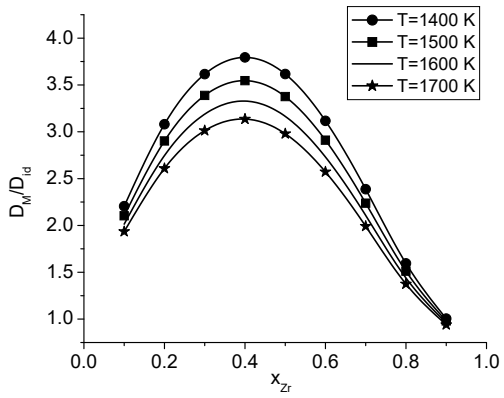

Figure 8: Compositional dependence of D_M/D_{id} for Cu–Zr liquid alloy in the temperature range 1400-1700 K.

The calculated values of D_M/D_{id} are found to be greater than 1 at all concentrations at 1400 K, melting temperature. This result reveals that the system shows hetero-coordinating tendency. Meanwhile, the calculated values of D_M/D_{id} decreases with gradual increase in temperature of the system. The calculated values of $D_M/D_{\mathrm{id}} < 1$ in the range $x_{\mathrm{Zr}} > 0.8$ and T>1400 K indicating the transformation from ordering to segregating nature, Figure 8. Thus, the nature of temperature-dependent mixing tendency of the system predicted by thermodynamic and structural functions are in accordance with each other.

3.3 Surface properties

The surface tension (σ) and surface concentration (x_i^s) of the system have been computed using Equations (15-21) and the parameters in Table 2. The above determined values of thermodynamic parameters have been used for the purpose. The calculated values of x_i^s are plotted as a function of concentration in Figures 9.

It can be observed that the calculated values of $x^s_{\mathrm{Zr}}<x_{\mathrm{Zr}}$ and $x^s_{\mathrm{Cu}}>x_{\mathrm{Cu}}$ in the entire composition range at 1400 K, Figure 9. These results have been occurred as the surface tension of Cu ($\sigma_{\mathrm{Cu}} = 1.293$ Nm^{-1}) is less than that of Zr ($\sigma_{\mathrm{Zr}} = 1.633$ Nm^{-1}) at this temperature. Hence, Cu atoms segregate in the surface phase whereas Zr atoms remain in the bulk phase of the liquid alloy.

Table 2: Surface tension and density of each component of liquid alloy [23]

Surface tension [Nm^{-1}]
$\sigma^0_{\mathrm{Zr}} = 1.459 - 0.00024(T - 2128)$
$\sigma^0_{\mathrm{Cu}} = 1.303 - 0.00023(T - 1356)$
Density [kgm^{-3}]
$\rho^0_{\mathrm{Zr}} = 6240 - 0.29(T - 2128)$
$\rho^0_{\mathrm{Cu}} = 8000 - 0.8(T - 1356)$

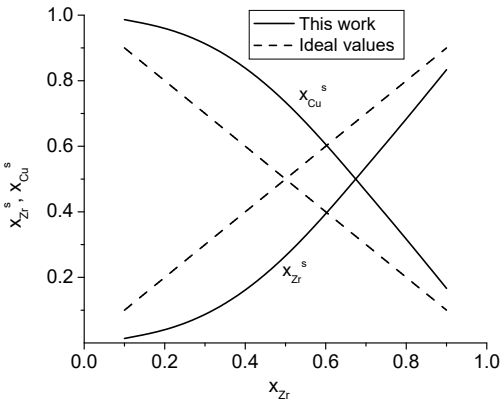

Figure 9: Compositional dependence of calculated values of x^s_{Zr} and x^s_{Cu} for Cu–Zr liquid alloy at 1400 K.

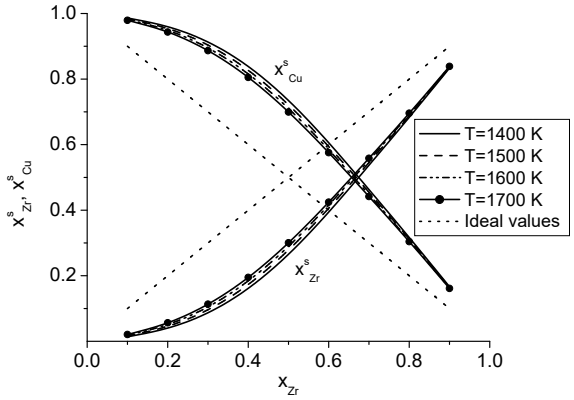

Figure 10: Calculated values of x^s_{Zr} and x^s_{Cu} for Cu–Zr liquid alloy at different temperatures.

The values of x^s_{Zr} and x^s_{Cu} have also been computed in the temperature range 1400-1700 K. It can be observed that the calculated values of x^s_{Zr} are found to increase while those of x^s_{Cu} are found to decrease at higher temperatures. Both of these values get closure to their respective bulk concentrations or ideal values as the temperature of the system is increased, Figure 10. Thus, Cu atoms move towards the bulk phase whereas Zr atoms move towards the surface phase at elevated temperatures.

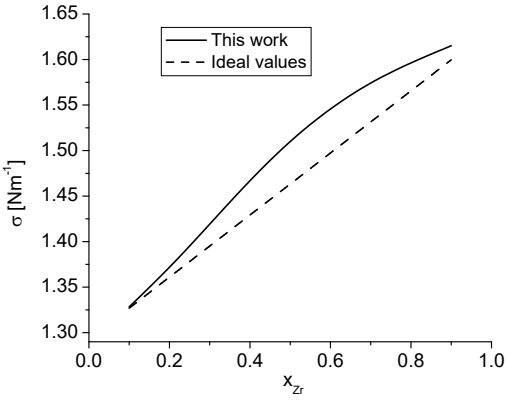

Figure 11: Calculated values of σ for Cu–Zr liquid alloy at 1400 K.

The computed values of σ of the system is found to be less than its ideal values. Moreover, the surface tension of the system gradually increases with increase in concentration of Zr, Figure 11. The temperature-dependent variation of σ of the system is as shown in Figure 12. The surface tension of the system decreases gradually and linearly with an increase in temperature of the system.

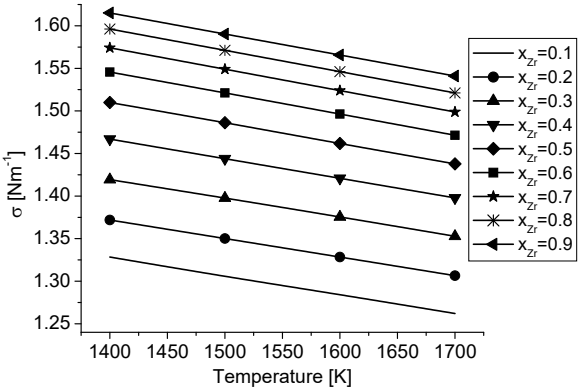

Figure 12: Calculated values of σ for Cu–Zr liquid alloy at different temperatures.

4 Conclusion

The computed values of the thermodynamic properties of the system using the best fit values of the model parameters of the work are found to be consistent with the reference database. The Cu-Zr system is found to be weakly interacting in nature and shows complete ordering tendency at its melting temperature, 1400 K. With an increase in temperature of the system, it shows transformation from ordering to segregating nature in the concentrations range $x_{\mathrm{Zr}} > 0.8$ and T>1400 K. The results predicted by the thermodynamic and structural functions are in accordance with each other. The surface tension of the system is found to increase with an increase in concentration of Zr. Moreover, the surface tension decreases gradually and linearly at elevated temperatures.

References

[1] O.J. Kleppa and S. Watanabe. Thermochemistry of alloys of transition metals: Part III. Copper-Silver,-Titanium, Zirconium, and-Hafnium at 1373 K. *Metallurgical Transactions B*, 13:391–401, 1982.

[2] K. Yamaguchi, Y.C. Song, T. Yoshida, and K. Itagaki. Thermodynamic investigation of the cu–zr system. *Journal of alloys and compounds*, 452(1):73–79, 2008.

[3] A.I. Zaitsev, N.E. Zaitseva, Y. P. Alekseeva, E.M. Kuril'chenko, and S.F. Dunaev. Thermodynamic properties of melts and phase equilibria in the copper–zirconium system. *Inorganic materials*, 39:816–825, 2003.

[4] D. S. Kanibolotsky, O. A. Bieloborodova, and V. V. Lisnyak. Thermodynamic properties

of liquid germanium–yttrium alloys. *Thermochimica acta*, 433(1-2):13–18, 2005.

[5] A.A. Nayeb-Hashemi and J.B. Clark. The Cu-Mg (copper-magnesium) system. *Bulletin of Alloy Phase Diagrams*, 5(1):36–43, 1984.

[6] A.B. Bhatia and W.H. Hargrove. Concentration fluctuations and thermodynamic properties of some compound forming binary molten systems. *Physical Review B*, 10(8):3186, 1974.

[7] A. B. Bhatia and R. N. Singh. A quasi-lattice theory for compound forming molten alloys. *Physics and Chemistry of Liquids an International Journal*, 13(3):177–190, 1984.

[8] D. Adhikari, S. K. Yadav, and L. N. Jha. Thermo-physical properties of mg-tl melt. *Journal of Basic and Applied Research International*, 9(2):103–110, 2015.

[9] S. K. Yadav. Assessment of Thermodynamic and Structural Properties of Al–Er liquid Alloy at Different Temperatures. *The Journal of Knowledge and Innovation*, pages 66–74, 2023.

[10] D. Adhikari, BP Singh, IS Jha, and BK Singh. Chemical ordering and thermodynamic properties of HgNa liquid alloys. *Journal of Non-Crystalline Solids*, 357(15):2892–2896, 2011.

[11] I. Ansara, A. T. Dinsdale, and M. H. Rand. *Thermochemical database for light metal alloys*. Office for Official Publications of the European Communities, 1998.

[12] J. A. V. Butler. The thermodynamics of the surfaces of solutions. *Proceedings of the Royal Society of London. Series A, Containing Papers of a Mathematical and Physical Character*, 135(827):348–375, 1932.

[13] G. Kaptay. Improved derivation of the butler equations for surface tension of solutions. *Langmuir*, 35(33):10987–10992, 2019.

[14] S.K. Yadav, M. Gautam, and D. Adhikari. Mixing properties of Cu–Mg liquid alloy. *AIP Advances*, 10(12), 2020.

[15] S.K. Yadav, L.N. Jha, and D. Adhikari. Thermodynamic and structural behaviour of Mg–Ga melt at 923 K. *Journal of Advanced Physics*, 3(3):248–253, 2014.

[16] J.M. Cowley. An approximate theory of order in alloys. *Physical Review*, 77(5):669, 1950.

[17] R. Novakovic. Thermodynamics, surface properties and microscopic functions of liquid Al–Nb and Nb–Ti alloys. *Journal of Non-Crystalline Solids*, 356(31-32):1593–1598, 2010.

[18] D. Adhikari, I.S. Jha, and B.P. Singh. Structural asymmetry in liquid Fe–Si alloys. *Philosophical Magazine*, 90(20):2687–2694, 2010.

[19] L. S. Darken and R. W. Gurry. Physical chemistry of metals. *(No Title)*, 1953.

[20] G. Kaptay. Partial surface tension of components of a solution. *Langmuir*, 31(21):5796–5804, 2015.

[21] Sharma P. Koirala R.P. Dhungana A.and Adhikari D. Yadav, S.K. Mixing properties of Ni–Al liquid alloys at different temperatures. *Bibechana*, 16:106, 2018.

[22] IS Jha, D Adhikari, J Kumar, and BP Singh. Anomaly in mixing properties of lithium–magnesium liquid alloy. *Phase Transitions*, 84(11-12):1075–1083, 2011.

[23] E.A. Brandes and G.B. Brook. *Smithells metals reference book*. Elsevier, 2013.

[24] S.K. Yadav, L.N. Jha, and D. Adhikari. Thermodynamic, structural, transport and surface properties of Pb-Tl liquid alloy. *Bibechana*, 13:100, 2016.

[25] O. Redlich and A. T. Kister. Algebraic representation of thermodynamic properties and the classification of solutions. *Industrial & Engineering Chemistry*, 40(2):345–348, 1948.